Pergamon

Bioorganic & Medicinal Chemistry 8 (2000) 275–284

BIOORGANIC & MEDICINAL CHEMISTRY

Stereo-Enriched Phosphorothioate Oligodeoxynucleotides: Synthesis, Biophysical and Biological Properties

Dong Yu,[a] Ekambar R. Kandimalla,[a] Allysen Roskey,[a] Qiuyan Zhao,[a] Lihong Chen,[b] Jiangdong Chen[b] and Sudhir Agrawal[a,*]

[a]*Hybridon, Inc., 155 Fortune Boulevard, Milford, MA 01757, USA*
[b]*Department of Microbiology, Louisiana State University Medical Center, New Orleans, LA 70112, USA*

Received 22 July 1999; accepted 7 October 1999

Abstract—Stereo-enriched [Rp] and [Sp]-phosphorothioate oligodeoxynucleotides are synthesized using oxazaphospholidine derivatized monomers. Three different designs of phosphorothioate oligodeoxynucleotides (PS-oligos), (i) stereo-enriched all-[Rp] or all-[Sp] PS-linkages, (ii) stereo-random mixture of PS-linkages, and (iii) segments containing certain number of stereo-enriched [Rp] and [Sp] PS-linkages ([Sp-Rp-Sp] or [Rp-Sp-Rp]), have been studied. Thermal melting studies of these PS-oligos with RNA complementary strands showed that the binding affinities are in the order [Rp] > [Sp-Rp-Sp] = [Rp-Sp-Rp] > stereo-random > [Sp]. Circular dichroism (CD) studies suggest that the stereochemistry of the PS-oligo does not affect the global conformation of the duplex. The in vitro nuclease stability of these PS-oligos is in the order [Sp] > [Sp-Rp-Sp] > stereo-random > [Rp]. The RNase H activation is in the order [Rp] > stereo-random > [Rp-Sp-Rp] > [Sp] > [Sp-Rp-Sp]. Studies in a cancer cell line of PS-oligos targeted to MDM2 mRNA showed that all oligos had similar biological activity under the experimental conditions employed. Protein- and enzyme-binding studies showed insignificant stereo-dependent binding to proteins. The [Sp] and [Sp-Rp-Sp] chimeric and stereo-random PS-oligos that contained a CpG motif showed higher cell proliferation than [Rp] PS-oligo of the same sequence.

Introduction

Phosphorothioate oligodeoxynucleotides (PS-oligos) are being evaluated in clinical trials for efficacy against viral and inflammatory diseases and cancers.[1,2] As a result of sulfur substitution for a non-bridging oxygen on phosphorus, chirality is introduced at the phosphorus center resulting in [Rp] and [Sp] diastereomers.[3] Our previous studies using enzymatically synthesized stereo-regular [Rp] PS-oligo in comparison with a stereo-random PS-oligo showed stereochemistry-dependent biophysical and biochemical properties.[4] Subsequent studies of chemically synthesized stereo-regular [Rp] PS-oligos further confirmed higher binding affinity to the target RNA, better activation of RNase H enzyme, and faster degradation by 3′-exonucleases than stereo-regular [Sp] and stereo-random PS-oligos.[5,6] Stereo-regular PS-oligos showed different properties of triple helix formation in Pu.Pu:Py and Py.Pu:Py motifs.[7] In addition, certain polymerases and nucleases interact and exert action on PS-oligos in a diastereomeric-selective fashion.[3] Although there are no detailed comparative structural studies on stereo-regular [Sp] and [Rp] phosphorothioate containing duplexes, molecular modeling studies of the heteroduplexes containing stereo-regular [Sp] and [Rp] phosphorothioate strands suggested that in the [Sp] stereomer sulfur atom is directed towards the minor groove and in the [Rp] stereomer sulfur atom is pointed into the major groove of the heteroduplex.[8] In vivo pharmacokinetic and safety profiles of stereo-regular PS-oligos are not known because of the lack of convenient synthetic methods to prepare diastereomerically pure PS-oligos in sufficient quantities required for these studies.

PS-oligos are obtained as a mixture of 2^n diastereomers, (n is number of phosphorothioate internucleoside linkages) on an automated DNA synthesizer using β-cyanoethylphosphoramidite chemistry. Diastereomerically pure PS-oligos can be obtained by HPLC purification of random mixtures obtained by β-cyanoethylphosphoramidite chemical synthesis.[9] Such a methodology, however, is limited to pentamer or shorter PS-oligos

Keywords: anticancer; antisense; oligonucleotides; phosphorothioates; stereo-enriched.
*Corresponding author. Tel.: +1-508-482-7000; fax: +1-508-482-7692; e-mail: sagrawal@hybridon.com

0968-0896/00/$ - see front matter
PII: S0968-0896(99)00275-8

and the yields of stereo-regular isomers obtained does not provide quantities required for detailed studies. In recent years efforts have been focused on developing methods for the synthesis of stereo-regular PS-oligos.[6,10–14] Nucleoside oxathiaphospholane synthons have been developed and used for stereoselective synthesis of PS-oligos in recent years.[6,11] This approach, however, requires prior chromatographic separation of the individual P-diastereomers of nucleoside oxathiaphospholane synthons, which are formed in 55:45 ratio.[11] Nucleoside oxathiaphospholane synthons require longer coupling times than standard β-cyanoethylphosphoramidite coupling cycles for efficient synthesis of stereo-regular PS-oligos. In addition, the presence of unprotected phosphorothioate groups generated during the coupling cycles may potentially lead to the formation of side products during oligonucleotide chain elongation.[11]

In an effort to develop cost-effective and efficient methodologies for the stereo-controlled synthesis of phosphorothioate oligonucleotides, we recently reported the use of (*S*)-(+)-2-pyrrolidine-methanol (L-prolinol), and (*R*)-(−)-2-pyrrolidine-methanol (D-prolinol) for the synthesis of 3′-bicyclic oxazaphospholidine nucleosides.[15] Importantly, the reaction between the chlorophosphite reactant and the *N*-protected 5′-*O*-DMTr nucleoside gives a single diastereomer of bicyclic oxazaphospholidine nucleoside minimizing further separation of the two diastereomers. Using oxazaphospholidine derivatized nucleosides and employing automated solid phase DNA synthesis, we obtained stereo-enriched PS-dinucleotides.[15] We have recently extended this chemistry for the synthesis of PS-2′-*O*-methyl dinucleotides.[16]

In continuation, now we have extended the methodology for the synthesis of longer PS-oligos (up to 20-mers) containing stereo-enriched all [Rp] or all [Sp] linkages. We have also synthesized PS-oligos containing a central [Rp] segment and [Sp] segments on either side or vice versa using appropriate oxazaphospholidine nucleoside building blocks. Our goal is to explore the potential of stereo-enriched PS-oligos as antisense agents. We report here, the results of stereo-enriched PS-oligos for their target binding affinity by UV thermal melting studies, and the effect on the global conformation of the duplexes of the stereo-enriched PS-oligos with the RNA and DNA target strands by circular dichroism (CD) studies. We have also examined the nuclease stability towards snake venom phosphodiesterase, human DNA polymerase I, and human serum, RNase H activation, protein binding, cell proliferation, and biological activity in cell cultures, and compared the results with a stereo-random PS-oligo of the same sequence and length synthesized by using β-cyanoethylphosphoramidite chemistry.

Results and Discussion

Synthesis

We have examined whether the new chemistry could be extended to synthesize [Rp] and [Sp] PS-oligos of varying lengths and base compositions (Scheme 1). Stereoselectivity of coupling of each 5′-DMTr-protected oxazaphospholidine monomer (**a**–**h**) to a thymine nucleoside attached to a controlled pore glass (CPG) support was determined by isolating and analyzing the dimers on HPLC as reported earlier for a TT dimer.[15] Stereoselectivity of each dimer is shown in Table 1. These data suggest that the stereo-selectivity of the coupling is dependent on the nucleoside base.

Both [Rp] and [Sp] PS-oligos were synthesized on CPG solid support using appropriate 5′-DMTr-protected oxazaphospholidine monomers (Scheme 1). The stereo-random PS-oligo was synthesized using β-cyanoethylphosphoramidite chemistry producing a diastereomeric mixture. The chimeric PS-oligos containing [Sp] segments at the 3′ and 5′-ends and [Rp] segments in the middle (or vice versa) were synthesized using appropriate oxazaphospholidine monomers (Table 2). The stereo-enriched PS-oligos were deprotected and purified by polyacrylamide gel electrophoresis (PAGE). The purity of the oligonucleotides was determined by ^{31}P NMR, reverse-phase HPLC, capillary gel electrophoresis (CGE) and denaturing PAGE. Diastereomeric purity was assessed by nuclease (snake venom phosphodiesterase and nuclease P1) digestion assays as described earlier.[3] The oligonucleotide sequences synthesized are shown in Table 2. We have used two different sequences that have been studied extensively in the past. The PKA sequence shown in Table 2 is complementary to an 18-base long site on the mRNA of regulatory subunit Iα (RIα) of human protein kinase A (PKA).[17,18] The MDM2 oligo sequences (Table 2) are complementary to a 20-base long sequence on the mRNA of human MDM2 gene.[19]

UV thermal melting studies

UV thermal melting studies of the duplexes of PS-oligos with their target RNA and DNA strands were carried out. Thermal melting curves of the duplexes of PS-oligos **1**–**4** with the target RNA are shown in Figure 1A and the T_ms measured for each PS-oligo duplex are shown in Table 3. These data suggest that [Rp], [Sp] and stereo-random PS-oligos have different binding affinities to the target RNA. The [Rp] PS-oligo **2** formed a duplex with the RNA target that has a T_m of 67.7 °C (Table 3). The duplex of the [Sp] PS-oligo **3** and the RNA target has a T_m 8.7 °C lower than that obtained for the duplex of **2** and the RNA target. These data suggest that [Rp] configuration is more favorable for binding to the RNA than the [Sp] configuration; these findings are consistent with earlier reports.[3–6] The duplex of the stereo-random PS-oligo **1** and the RNA target has a T_m that is intermediate to the T_ms of the duplexes of [Rp] (**2**) and [Sp] (**3**) PS-oligos of the same sequence and the RNA target. The thermal stability of the duplex of chimeric PS-oligo **4** and the RNA target suggests that the six [Sp] linkages (three at each end) reduced T_m only by 1.3 °C compared to [Rp] PS-oligo **2** duplex with the same target strand.

The duplexes of PS-oligos **1**–**4** with the DNA target have similar T_ms (60.3 ± 1.0 °C) (Table 3). The thermal

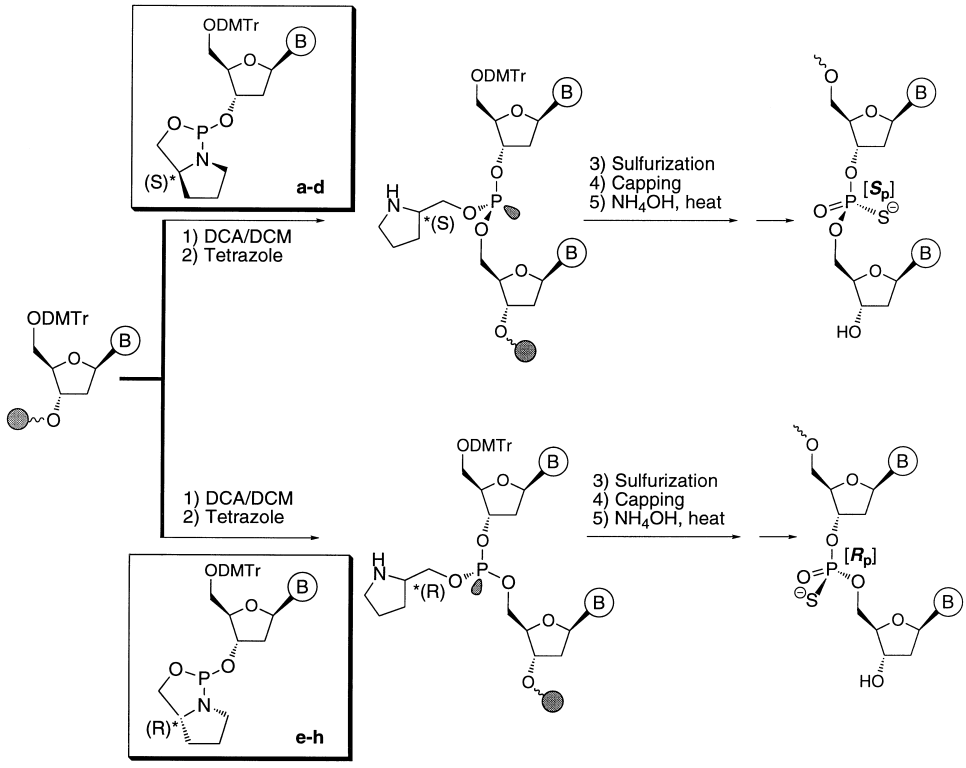

Scheme 1. Synthesis of stereo-enriched PS-oligos. **a**–**d** and **e**–**h** are obtained from (*S*)-(+)-2-pyrrolidine methanol and (*R*)-(−)-2-pyrrolidine methanol, respectively. (1) The 5′-*O*-DMTr group of the nucleobase attached to CPG solid support is cleaved by dichloroacetic acid (DCA) in dichloromethane (DCM). (2) Coupling of the incoming 5′-*O*-DMTr bicyclic oxazaphospholidine nucleoside **a**–**d** or **e**–**h**, tetrazole is an activator; B stands for base, **a** and **e** = *T*; **b** and **f** = A^{bz}; **c** and **g** = G^{ibu}; **d** and **h** = C^{bz}. (3) Sulfurization (oxidation) was carried out with 3H-1,2-benzodithiole-3-one-1,1-dioxide. (4) Capping of the unreacted hydroxy groups. (5) At the end of the synthesis, PS-oligos were cleaved, deprotected and purified as described in Experimental.

Table 1. Stereo-selectivity of synthesis of dinucleotide phosphorothioates

Bicyclic oxazaphospholidine nudeoside monomer	Dimer[a]	Ratio of stereo-selectivity[b] [Rp]:[Sp]
a	5′-d**T**T	12:88
b	5′-d**A**T	14:86
c	5′-d**G**T	10:90
d	5′-d**C**T	13:87
e	5′-d**T**T	91:9
f	5′-d**A**T	93:7
g	5′-d**G**T	92:8
h	5′-d**C**T	92:9

[a]Base shown as plane letter indicates CPG attached, the incoming nucleoside (**a**–**h**) is shown in bold.
[b]Stereo-selectivity of coupling of each nucleoside synthon in dimer is determined by analytical HPLC as described in Experimental.

melting studies of the duplexes of PS-oligos with the DNA target strand suggest that binding to the DNA complementary strand is less dependent on the stereochemistry compared to the RNA complementary strand.

Similar thermal melting trends were observed for duplexes of MDM2 PS-oligos **5**–**10** with the RNA target (Table 3). The difference in the T_ms of duplexes of [Rp] and [Sp] MDM2 PS-oligos was not as pronounced as in the case of PKA oligos. This could be as a result of the difference in the base composition of the two oligonucleotide sequences. The PKA sequence contains 72% G and C bases, while the MDM2 sequence contains only 50% G and C bases.

CD studies

CD experiments have been carried out in order to examine whether the duplexes of the two diastereomers with RNA and DNA targets exhibit any differences in the global conformations. The CD spectra of the duplexes of PS-oligos **1**–**4** with the RNA/DNA strands are shown in Figure 1B and C. The duplexes of both the [Rp]. [Sp] (**2** and **3**) and stereo-random (**1**) PS-oligos with the DNA target sequence have similar CD spectral characteristics with slight differences in band intensities (Fig. 1B). The spectra of the duplexes of PS-oligos with the DNA target strand exhibited B-type spectral characteristics. We did not observe a C-type conformational CD spectrum for the duplex of [Sp] PS-oligo and DNA target strand as reported for a duplex of an [Sp] phosphorothioate pentamer and its DNA complementary strand.[9]

The CD spectra of the duplexes of the PS-oligos and the RNA target showed a larger positive CD band at around 267 nm and two negative CD bands at around 235 (shallow) and 210 nm (deep) characteristic of A-type conformation (Fig. 1C).[20,21] The CD intensities of the three duplexes of the PS-oligos with the RNA

Table 2. Oligonucleotide sequences

No.	PS-oligo[a]	Sequence
PKA oligos		
1	SR	5′-d(GCGTGCCTCCTCACTGGC)-3′
2	[Rp]	5′-d(GRCRGRTRGRCRCRTRCRCRTRCRARCRTRGRGRC)-3′
3	[Sp]	5′-d(GsCsGsTsGsCsCsTsCsCsTsCsAsCsTsGsGsC)-3′
4	[Sp-Rp-Sp]-chimer	5′-d(GsCsGsTRGRCRCRTRCRCRTRCRARCRTsGsGsC)-3′
MDM2 oligos		
5	SR	5′-d(TGACACCTG-ITCTCACTCAC)-3′
6	[Rp]	5′-d(TRGRARCRARCRCRTRGRTRTRCRTRCRARCRTRCRARC)-3′
7	[Sp]	5′-d(TsGsAsCsAsCsCsTsGsTsTsCsTsCsAsCsTsCsAsC)-3′
8	[Rp-Sp-Rp]-chimer	5′-d(TRGRARCRARCRCRTsGsTsTsCsTRCRARCRTRCRARC)-3′
9	[Sp-Rp-Sp]-chimer	5′-d(TsGsAsCsARCRCRTRGRTRTRCRTRCRAsCsTsCsAsC)-3′
10	Sr control	5′-d(TGACTCTTGTACTTACTCAC)-3′
Oligos containing CpG motif		
11	SR	5′-d(TCCATGA*CG*TTCCTGATGC)-3′
12	[Rp]	5′-d(TRCRCRARTRGRARC*R*GRTRTRCRCRTRGRARTRGRC)-3′
13	[Sp]	5′-d(TsCsCsAsTsGsAs*CsGs*TsTsCsCsTsGsAsTsGsC)-3′
14	[Sp-Rp-Sp]-chimer	5′-d(TsCsCsARTRGRARC*R*G*R*TRTRCRCRTRGRAsTsGsC)-3′

[a]Stereo-random (SR) represents a PS-oligo synthesized by β-cyanoethylphosphoramidite chemistry, containing 2^n diastereomers (n = number of phosphorothioate internucleoside linkages). Chimer represents stereo-enriched PS-oligo that contains a specific number of [Sp] or [Rp] phosphorothioate linkages as represented with R for [Rp] and S for [Sp] linkages. The CpG motif in oligos **11**–**14** is shown in italics. Underlined bases in SR control sequence represent mismatched bases.

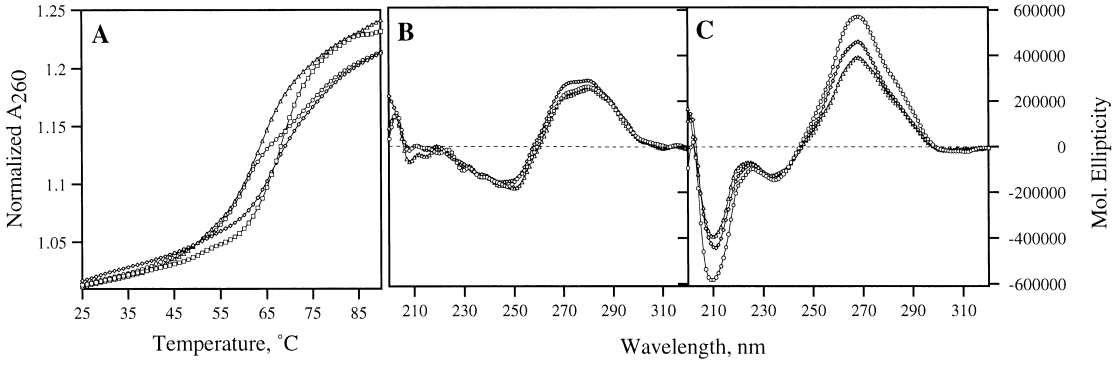

Figure 1. (A) UV thermal melting curves of the duplexes of PS-oligos **1** (△), **2** (◇), **3** (○), and [Sp-Rp-Sp] chimer **4** (□) with the target RNA. CD spectra of the duplexes of PS-oligos **1**–**3** with the target DNA (B) and RNA (C) sequences. In both panels B and C: ◇ (**1**), ○ (**2**) and △ (**3**).

target strand are in the order [Rp] > stereo-random > [Sp]. These results suggest that the stereochemistry of the PS-oligo backbone does not alter the global conformation of the duplexes formed with RNA/DNA target strands.[4,20–22]

Nuclease stability of stereo-enriched PS-oligos

We have studied the stability of PS-oligos **5**–**9** against DNA polymerase I and SVPD and in human serum. Figure 2A shows SVPD digestion of oligos **5**–**9**. From the digestion profiles, it is clear that SVPD digests [Rp] diastereomer selectively over [Sp] diastereomer.[3] The [Sp] PS-oligo **7** is more stable than [Rp] PS-oligo **6**. The stereo-random PS-oligo **5** has a stability intermediate to the stability of [Sp] and [Rp] PS-oligos. The extent of degradation of PS-oligos **5**–**7** suggest percentage of [Rp] (degraded bands) and [Sp] (intact oligo band) population in each oligo. The chimeric PS-oligo **9** ([Sp-Rp-Sp]) with [Sp] linkages at the 3′- and 5′-ends is as stable as the [Sp] PS-oligo. The PS-oligo **8** with [Rp] linkages at the ends is digested as in the case of [Rp] PS-oligo **6**. Note the less intense bands in the middle of the gel in the lanes corresponding to oligo **8**, which contained [Sp] linkages in that region of the sequence. The PS-oligos **1**–**4** showed similar stability as observed with oligos **5**–**7** against SVPD as studied by CGE (data not shown).

Figure 2B shows digestion of oligos **5**–**9** in the presence of DNA polymerase I. DNA polymerase I exhibits 3′-exonuclease activity under the appropriate experimental conditions. The digestion profiles in Figure 2B suggest that DNA polymerase has diastereomeric selectivity similar to that of SVPD. The extent of degradation, however, is weaker than in the case of SVPD.

The two nucleases used in these studies showed diastereomeric-dependent activity. To examine if human serum nucleases exhibit any selectivity for [Rp] and [Sp] diastereomers and study the stability of PS-oligos **5**–**9** against serum nucleases, we incubated these oligos in human serum and examined the degradation pattern of each PS-oligo on denaturing polyacrylamide gels. Figure 3 shows the stability of PS-oligos in human serum at different time intervals. In human serum also, [Sp] PS-oligo **7** was more stable than the [Rp] PS-oligo **6**, as was

Table 3. T_ms of the duplexes of PS-oligos with the RNA and DNA target strands

PS-oligo[b]		T_m (°C)[a] with RNA (ΔT_m)[c]	T_m (°C)[a] with DNA (ΔT_m)
PKA oligos			
1	SR	63.3 (—)	59.2 (—)
2	[Rp]	67.7 (+4.4)	61.3 (+2.1)
3	[Sp]	59.0 (−4.3)	59.3 (+0.1)
4	[Sp-Rp-Sp]-chimer	66.4 (+3.1)	60.6 (+1.4)
MDM2 oligos			
5	SR	57.8 (—)	58.6 (—)
6	[Rp]	58.8 (+1.0)	nd[d]
7	[Sp]	56.0 (−1.8)	nd
8	[Rp-Sp-Rp]-chimer	57.5 (−0.3)	nd
9	[Sp-Rp-Sp]-chimer	57.3 (−0.5)	nd
10	SR control	23.3 (−34.5)	26.5 (−32.1)
Target RNAs			
For PKA oligos	5′-ACCGCC**GCCAGUGAGGAGGCACGC**AGCCUU-3′[e]		
For MDM2 oligos	5′-CU**GUGAGUGAGAACAGGUGUCA**CCU-3′		

[a]See Experimental for buffer conditions and oligo concentrations.
[b]Sequences of PS-oligos are shown in Table 1.
[c]The numbers shown in parentheses (ΔT_m) are the differences in the T_m and relative to the T_m of the duplex of stereo-random PS-oligo with the target.
[d]nd, not determined.
[e]The complementary sites for the corresponding antisense oligos in the target RNA sequences are shown in bold face.

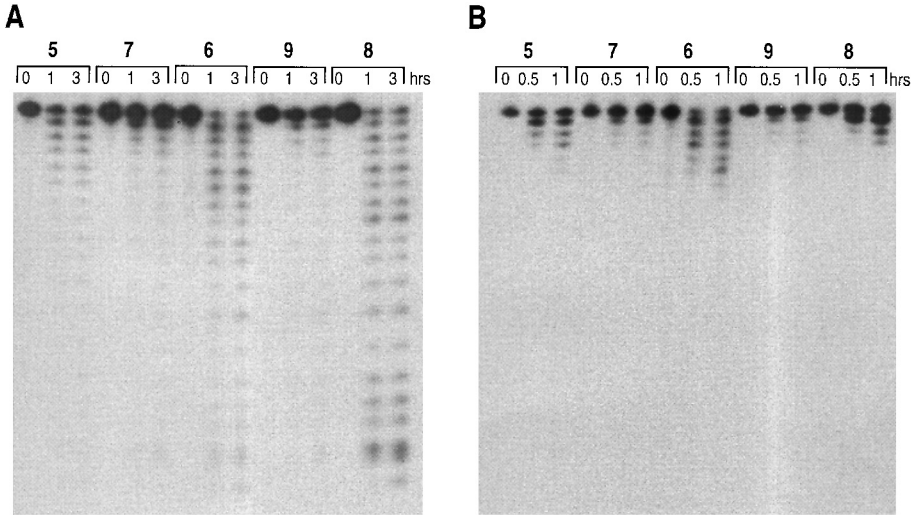

Figure 2. Autoradiograms showing (A) SVPD and (B) DNA polymerase I digestion of PS-oligos **5**–**9** at different time points.

observed earlier. Importantly, the [Sp-Rp-Sp] chimeric PS-oligo **9** was as stable as [Sp] PS-oligo in human serum.

RNase H activity of stereo-enriched PS-oligos

Figure 4A shows RNase H hydrolysis of RNA in the presence of PS-oligos **5**–**10**. RNA is cleaved in the presence of all PS-oligos, except stereo-random mismatched PS-oligo **10**, which has four mismatches. The results in Figure 4A show that the rate and pattern of RNase H cleavage is different in the presence of each PS-oligo. In general, no intact RNA was left at the 15-min time point (except in the case of chimeric PS-oligo **9**). The presence of stereo-random, [Rp], and [Sp] PS-oligos yielded similar RNA cleavage patterns. The rate of RNase H cleavage of RNA is dependent on the chirality at the phosphorus center. To assess the rate of RNase H hydrolysis of RNA in the presence of each PS-oligo, the intact RNA band in each lane was determined and plotted as percent RNA hydrolyzed at the 1- and 5-min time points (Fig. 4B). The efficiency of RNase H cleavage of RNA in the presence of PS-oligos is in the order: [Rp] > stereo-random > [Sp]. These results confirm earlier observations that [Rp] diastereomer activates RNase H better than [Sp] diastereomer.

Comparison of the RNA cleavage pattern in the presence of chimeric PS-oligos **8** and **9** suggest that cleavage is centered in the middle of the binding site with oligo **9** where the [Rp] segment is located. In the case of oligo **8**, the cleavage bands in the middle of the binding site are lighter, where the [Sp] segment is located, and the bands at the bottom of the gel are darker, where the

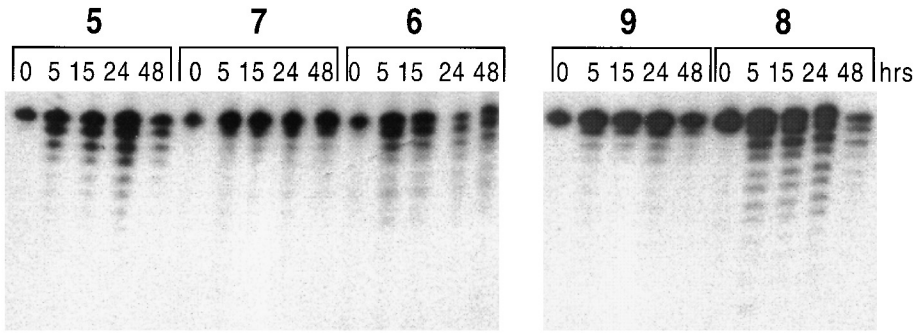

Figure 3. Autoradiograms showing digestion of PS-oligos **5**–**9** at different time points in human serum.

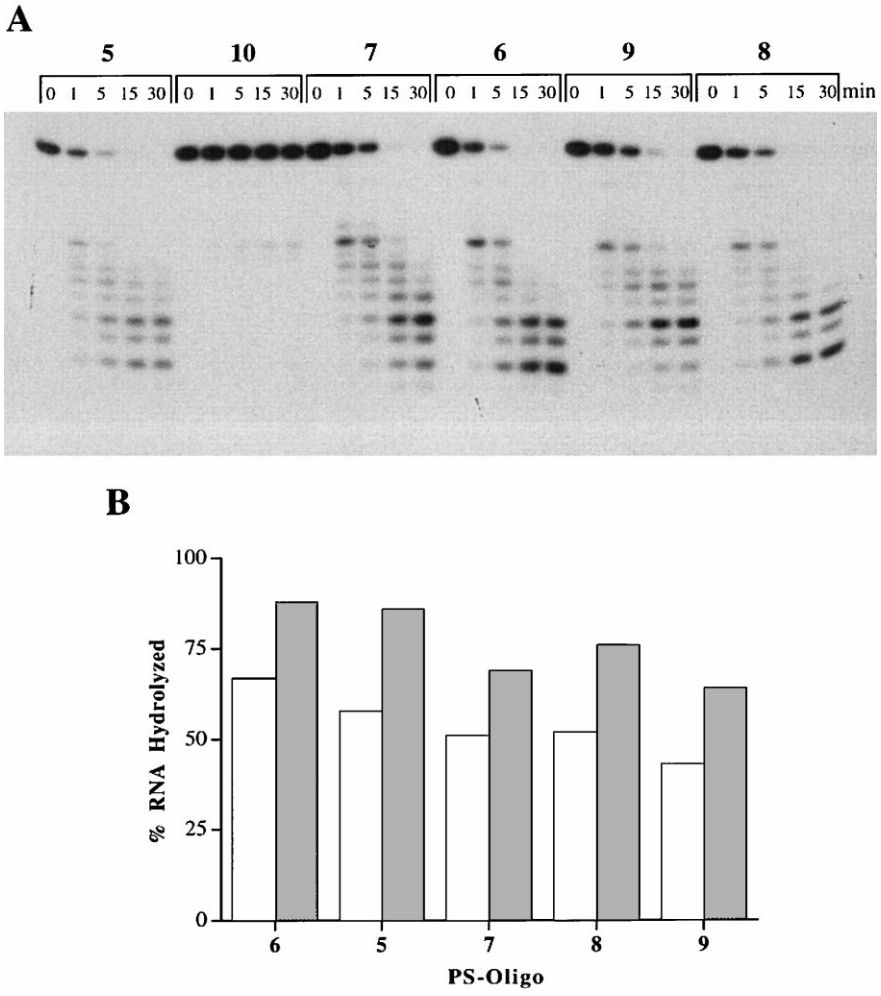

Figure 4. (A) An autoradiogram showing RNase H digestion profiles of the complementary RNA in the presence of PS-oligos **5**–**9** as labeled on top of the gel at different time points. The 0 time point lanes represent control RNA-PS-oligo duplex in the absence of RNase H. (B) A plot showing % of the target RNA hydrolyzed in the presence of each PS-oligo at 1 min (white bars) and 5 min (black bars) time points.

3′-end [Rp] segment is present. Figure 4B suggests that RNA cleavage is faster in the presence of chimeric oligo **8** than in the presence of oligo **9**. Our earlier studies with MBOs containing RNase H-activating segments either in the center (end-modified) or at the 3′- and 5′-ends with a central non-RNase H activating segment (centrally-modified) showed that RNase H cleavage of RNA is rapid in the presence of centrally modified MBOs.[23] In agreement with those results, the chimeric PS-oligo **8** containing more efficient RNase H activating [Rp] segments on either end ([Rp-Sp-Rp]) showed higher RNA hydrolysis.

Serum protein and enzyme binding of stereo-enriched PS-oligos

The 5′-end-labeled PS-oligos **5**–**9** were incubated with DNA polymerase I, recombinant HIV-reverse transcriptase, and human serum albumin (HSA), γ-globulins, and fibrinogen, and examined on non-denaturing

polyacrylamide gels for diastereomeric-dependent protein binding of stereo-enriched PS-oligos. All five oligos showed binding to proteins examined and the extent and strength of binding of these oligos was dependent on the protein used (data not shown) as reported for other proteins.[24,25] We did not observe significant differences in protein binding (for a given protein) of oligos **5**–**9** (data not shown). These results suggest that the protein binding of PS-oligos is not dependent on the nature of the diastereomeric isomer as has been observed with other stereo-regular PS-oligo sequences.[26]

Cell proliferation of stereo-enriched PS-oligos

PS-oligos containing CpG motif are known to induce cytokines, which has been associated with non-sequence-specific biological activity and side-effects.[27–30] To examine the role of [Rp] and [Sp] diastereomers of PS-oligos on cell proliferation, we synthesized PS-oligos (**11**–**14**) that contained a CpG motif (Table 2) and studied for their cell proliferative activity in cell cultures. The data are presented in Figure 5. The stereo-random and [Sp] PS-oligos showed higher proliferative activity than [Rp] PS-oligo. The PS-oligo **12** with [Rp] linkages did not induce significant cell proliferation under the experimental conditions. In order to examine whether the inability of [Rp] PS-oligo (**12**) to induce proliferation resulted from its lower stability against nucleases, we synthesized a chimeric PS-oligo (**14**, Table 2) with [Sp] linkages at both the ends and [Rp] linkages in the middle of the sequence. The linkage between C and G of the CpG motif was of the [Rp] type (see Table 2). This kind of chimeric design showed stability similar to that of [Sp] PS-oligo in nuclease stability studies. The data in Figure 4 suggest that this chimeric PS-oligo has cell proliferative activity comparable to that of [Sp] PS-oligo. These results suggest that the higher cell proliferative property of [Sp] diastereomer of [PS] oligos is probably the result of its higher stability against nucleases.

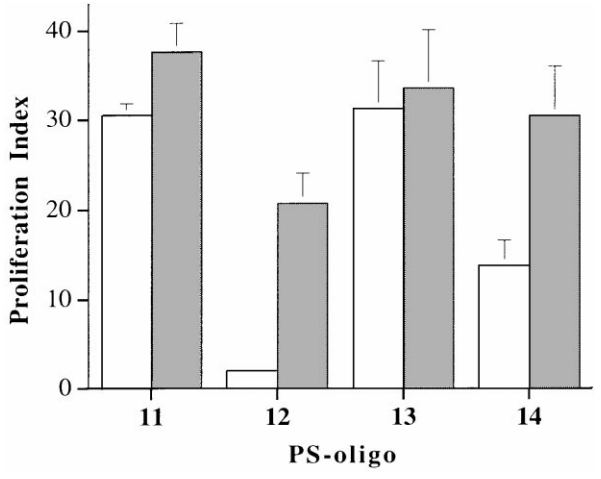

Figure 5. Effect of *p*-chirality on cell proliferative activity of PS-oligos (**11**–**14**) containing CpG motif. Each value is an average of two independent measurements. The white and dark shaded bars represent the concentrations of PS-oligos at 1.0 and 10.0 μM/mL, respectively.

Inhibition of MDM2 by stereo-enriched PS-oligos in cell cultures

PS-oligo **5** is complementary to MDM2 mRNA and has been studied in detail previously.[19] The earlier studies showed that PS-oligo **5** effectively down regulates MDM2 mRNA and its protein, which in turn stabilizes p53 and induces p21. The PS-oligo **5** has been used in several different cell lines. To determine p53 transcriptional activity, a p53-responsive luciferase reporter BP 100-luc containing the p53 binding site from the MDM2 gene was transfected into JAR cells with a neomycin-resistant marker plasmid as used previously.[19] The JAR-BP 100-luc cells were treated with different concentrations of PS-oligos and the luciferase activities were determined.

The [Sp] and [Rp] PS-oligos (**6** and **7**), [Sp-Rp-Sp] and [Rp-Sp-Rp] chimeric PS-oligos (**8** and **9**), and stereo-random PS-oligo (**5**) exhibited similar levels of down-regulation of MDM2, thereby activating p53 as detected by luciferase activity (Fig. 6). The control stereo-random PS-oligo (**10**) with four mismatches induced minimal luciferase activity (Fig. 6). These results suggest that under the experimental conditions used in cell cultures both [Rp] and [Sp] PS-oligos have activity similar to that of stereo-random PS-oligo.

There are contradicting reports in the literature about the biological activity of stereo-regular PS-oligos. A 15-mer-all [Rp] PS-oligo, which contained four contiguous Gs, has been reported to be consistently more active in inhibiting proliferation in cell culture experiments than were stereo-random and all [Sp] PS-oligos of the same sequence.[31] It was concluded that the higher efficacy observed with all-[Rp] PS-oligo was the result of increased hybridization efficiency to the target RNA

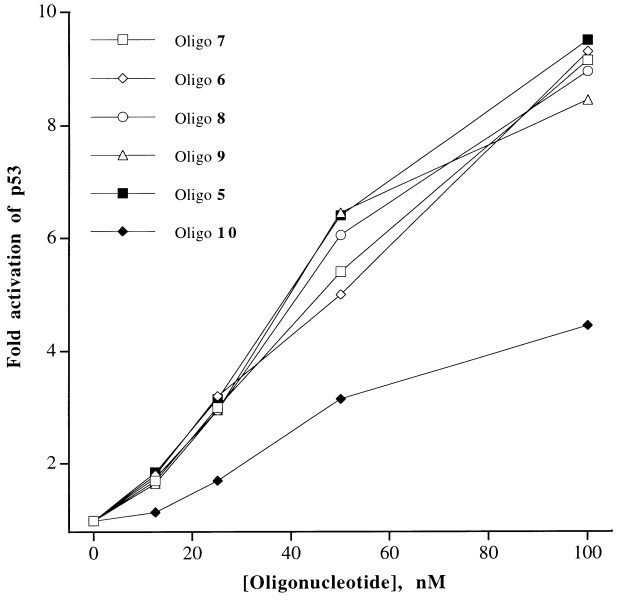

Figure 6. Inhibitory activity of MDM2 PS-oligos **5**–**10** in transfected JAR cells. Each value is an average of at least two independent experiments.

and greater ability to activate RNase H.[31] Higher efficacy of this [Rp] PS-oligo could also result from the increased stability of the oligonucleotide in serum as a result of higher-order structure formation by oligonucleotides that contain G-rich sequences.[32] A 16-mer all-[Sp] PS-oligo complementary to human PAI-1 mRNA has been shown to be more potent in cultures than stereo-random and all-[Rp] counterparts as a result of its higher stability against cellular and serum nucleases.[33,34] This oligonucleotide also contains a GAGGG sequence, however, which can potentially form a higher-order structure, although it was claimed not to form. The truncated and control oligonucleotides that were devoid of the GAGGG sequence were significantly less active, suggesting that this specific sequence motif is required for the observed biological activity.[33,34]

In spite of differences in the biophysical and biochemical properties of the two stereo-enriched PS-oligos, the oligonucleotides targeted to MDM2 mRNA did not show significant stereo-dependent differences in activity in cell cultures. The oligonucleotide sequence used in the present study does not contain motifs that promote formation of higher-order or self-complementary structures. This leaves the question, how would a less nuclease-resistant [Rp] diastereomer survive in cell culture medium and intracellularly, and exert comparable biological activity as that of [Sp] and stereo-random PS-oligos? In general, cationic lipids are used to facilitate transfection of oligonucleotides into cells in cell culture experiments. In the present study, lipofectin was used as a carrier for oligonucleotide delivery and the cells were incubated with oligos for 24 h. Negatively charged oligonucleotides form complexes with cationic molecules. The association of negatively charged oligonucleotides with lipids not only increases cellular uptake but also protects oligonucleotides from nuclease digestion.[35] Perhaps the lipids used in the cell culture experiments contributed to the longer half-life of [Rp] PS-oligo, which in turn could result in activity comparable to that of [Sp] and stereo-random PS-oligos.

Conclusions

We have shown that it is possible to synthesize stereo-enriched PS-oligos of varying lengths and base compositions using 5′-DMTr-protected oxazaphospholidine monomers. The present study showed that [Rp] PS-oligos have a higher binding affinity to the target RNA and greater RNase H activation, but lower stability against nucleases, than the stereo-random and [Sp] PS-oligos. The [Sp] PS-oligos have a lower binding affinity to the target RNA and lower RNase H activation, but greater stability against nucleases, than the stereo-random and [Rp] PS-oligos. In the present study we designed chimeric PS-oligos [Sp-Rp-Sp] and [Rp-Sp-Rp] in which advantageous properties of both the diastereomers can be combined. The cell culture studies showed that stereo-random, all-[Rp], all-[Sp], and chimeric PS-oligos have similar antisense activities. The cell-proliferatory activity of PS-oligos could be the result of the higher stability of the [Sp] diastereomer against nucleases. From these initial studies of chimeric PS-oligos, we propose that it might be possible to modulate pharmacokinetic and tissue disposition profiles of PS-oligos using chimeric designs, while retaining bioactivity similar to that of mixed-backbone oligonucleotides.[23] Further studies are ongoing to understand the impact of stereo-enriched PS-oligos on pharmacokinetic and stability, safety profiles, and in vivo activity.

Experimental

Preparation of bicyclic oxazaphospholidine nucleoside synthons

Synthesis of monomer **d**: to a cold solution of 5′-*O*-DMTr-2′-deoxy-*N*-benzoyl-cytidine (2.5 g; 3.96 mmol) in dry methylene chloride (~40 mL) and diisopropylethylamine (1 mL) was slowly added *p*-chloro-oxazaphospholidine (0.6 g; 3.96 mmol, derived from (*S*)-(+)-2-pyrrolidine methanol[15]) and stirred under argon at −78 °C for 30 min. The reaction mixture was allowed to come to ambient temperature and stirred overnight. The reaction was quenched by adding 100 mL of 5% ice-cold sodium bicarbonate solution. The product was extracted with methylene chloride (3×50 mL) and the combined organic extracts were dried over anhydrous sodium sulfate. The organic layer was evaporated and the solid **d** obtained was dried overnight in vacuo (yield 88%). The other monomers **a**–**c** were prepared similarly. For monomers **e**–**h**, phosphitylation agent was prepared from (*R*)-(−)-2-pyrrolidine methanol.[15] The yields were 90 ± 5%. The absolute configurations of **a**–**h** have not been assigned yet. The ^{31}P NMR spectra of monomers **a**–**h** were recorded on a Varian 600 MHz NMR spectrometer in $CDCl_3$ with 85% phosphoric acid as an external ^{31}P standard. ^{31}P NMR data (δ): **a**, 151.5; **b**, 153.9; **c**, 152.8; **d**, 152.6; **e**, 152.8; **f**, 152.4; **g**, 151.3; and **h**, 153.2.

Stereo-selectivity of the coupling of nucleoside monomers **a**–**h** to a thymidine nucleoside attached to a CPG support was determined by synthesizing and analyzing the dimers on HPLC as reported earlier.[15]

Oligonucleotide synthesis and purification

All oligodeoxynucleotides were synthesized on 1-μmol scale on a PerSeptive Biosystem's Expedite 8909 automated DNA synthesizer. Both [Rp] and [Sp] PS-oligos were synthesized on a CPG-solid support using appropriate 5′-DMTr-protected oxazaphospholidine monomers prepared as above. The stereo-random PS-oligo was synthesized using β-cyanoethylphosphoramidite chemistry producing a diastereomeric mixture. The chimeric PS-oligos containing [Sp] linkages at the 3′- and 5′-ends and [Rp] linkages in the middle (or vice versa) were synthesized using appropriate oxazaphospholidine monomers. The average coupling efficiency, as measured automatically by the synthesizer by trityl color determination at 498 nm at each detritylation step, was about 98%. The protected PS-oligos on CPG-solid support were treated with concentrated ammonium hydroxide at

65 °C for 16 h. The stereo-random PS-oligo with a 5′-DMTr group was purified by reverse phase HPLC on a C_{18} column and was subsequently detritylated with 80% acetic acid. Stereo-enriched PS-oligos were purified by preparative polyacrylamide gels. All the PS-oligos were desalted by dialysis against double distilled water. The concentrations were determined by UV absorbance measurement at 260 nm using extinction coefficients calculated by the nearest neighbor method. The yields of gel purified stereo-enriched PS-oligonucleotides were about 25% as further optimization of coupling conditions required.

UV absorbance melting experiments

The PS-oligos were mixed with either RNA or DNA target strands at a 1:1 molar ratio in a buffer containing 100 mM NaCl, 0.1 mM Na_2EDTA, and 10 mM sodium phosphate, pH 7.4. The total oligonucleotide concentration was 2 μM in a final volume of 1 mL. The samples were heated for 3 min and cooled slowly to room temperature prior to running the experiment. Absorbance melting curves were recorded on a Perkin–Elmer Lambda 20 UV–vis spectrometer equipped with Peltier-effect 6-cell holder. The temperature of the cell holder was controlled by an external PTP-6 Peltier System. The heating rate was 0.5 °C/min. Data were collected on a Dell OptiPlex GM5133 computer interfaced with the spectrometer and processed using the software supplied by Perkin–Elmer with the spectrometer. The melting temperatures (T_ms) of the duplexes were measured from first derivative plots obtained from thermal melting curves. Each experiment was repeated at least twice and the average was taken for T_m determinations. The reproducibility of the T_m values was within ±0.5 °C.

CD experiments

The same oligonucleotide sample solutions used for UV thermal melting studies were also used for CD experiments. The CD spectra were recorded on a Jasco J-710 spectropolarimeter with a 0.5 cm quartz cell attached to a Peltier thermal controller. The samples were equilibrated at 21 °C for 15 min before recording the spectra. Each spectrum was an average of 8 scans with the buffer blank subtracted, which was also an average of 8 scans and obtained at the same scan speed (100 nm/min). All the spectra were noise reduced using the software supplied by Jasco, and the molar ellipticities were calculated using the same software.

Nuclease digestion and PAGE

A small amount (85 pmol) of 5′-^{32}P-end-labeled PS-oligo was incubated with 2 units of snake venom phosphodiesterase (Boehringer Mannheim) in 30 μL of 10 mM Tris, pH 8.0 buffer containing 10 mM $MgCl_2$. An aliquot (7 μL) was removed at various time points and the reaction was stopped by adding 10 μL of formamide. The samples were analyzed on gels containing 20% acrylamide and 8 M urea. The extent of the nuclease hydrolysis was visualized by autoradiography.

A small amount (30 pmol) of 5′-^{32}P-end-labeled PS-oligo was incubated with 1.5 units of DNA polymerase I (Worthington Biochemical) in 20 μL of 50 mM Tris, pH 8.0 buffer containing 5 mM $MgCl_2$. An aliquot (5 μL) was removed at various time points and the reaction was stopped by adding 10 μL of formamide. The samples were analyzed on polyacrylamide gels as described above.

A small amount (30 pmol) of 5′-^{32}P-end-labeled PS-oligo was incubated with 100 μL of human serum (Bio Whittaker). An aliquot (25 μL) was removed at different time points and the sample was treated with 100 μg proteinase K (Boehringer Mannheim), 40 μL DNA extraction buffer (0.5% SDS, 10 mM NaCl, 20 mM Tris, pH 7.6, 10 mM EDTA) and 175 μL distilled water for 2 h at 60 °C. The oligos were extracted with 300 μL phenol and 300 μL chloroform and ethanol precipitated. The samples were dried, resuspended in 20 μL water and analyzed on polyacrylamide gels as described above.

RNase H experiments

Purified 25-mer RNA sequence (Table 2) complementary to the MDM2 antisense oligos was labeled with ^{32}P at the 5′-end using T4 polynucleotide kinase (New England Biolabs) and γ-^{32}P-ATP (Amersham) and used for RNase H assay as described earlier.[36] Briefly, the RNase H assay was carried out by forming a heteroduplex of labeled RNA (1 pmol) and the PS-oligos (1.0 pmol) in 10 μL of buffer containing 10 mM KCl, 5 mM $MgCl_2$, 0.1 mM DTT, 5% glycerol, 20 mM Tris–HCl, pH 7.5 and 40 units of RNase hihibitor (Boehringer Mannheim) was added and the total volume was adjusted to 30 μL. An aliquot of 5 μL was removed for 0 time point and 0.002 units of *Escherichia coli* RNase H (Amersham) was added and incubated at 37 °C. Aliquots (5 μL) were removed at different time points and the reaction was stopped by adding 5 μL formamide and freezing at −70 °C. The cleavage products were fractionated on polyacrylamide gels as described above.

In vitro cell proliferation assay

The cell proliferation assay was carried out as described earlier.[29] Briefly, spleen cell (4- to 5-week-old male CD1 mouse, 20–22 g; Charles River, Wilmington, MA) suspensions were prepared and plated in 96-well dishes at a density of 10^6 cells/mL in a final volume of 100 μL. The cells were incubated at 37 °C after the addition of 10 μL PS-oligo solution. After 44 h incubation, 1 μCi [^{3}H]thymidine (Amersham) was added and the cells were pulse labeled for another 4 h. The cells were harvested by an automatic cell harvester and the filters were counted using a scintillation counter. All experiments were carried out in triplicate.

Treatment of JAR-BP 100-luc cells by antisense oligonucleotides

The PS-oligos complementary to MDM2 mRNA were studied for their inhibitory activity in transfected JAR

cells as reported earlier.[19] The JAR cells were obtained from American Type Culture Collection. The JAR cells stably transfected with the p53-inducible BP 100-luciferase plasmid (JAR-BP100-luc) were treated with antisense oligonucleotides at different concentrations for 24 h. Luciferase activities in the treated cells were determined as described earlier.[19] The cells were cultured in DMEM with 10% fetal bovine serum (FBS). Before addition of antisense oligonucleotides, cells were supplemented with DMEM containing 1% FBS. Lipofectin (GIBCO/BRL) was incubated with serum-free DMEM medium at room temperature for 45 min and then mixed with antisense oligonucleotides for 10 min and added to the culture. The final concentration of lipofectin was 7 μg/mL and the final concentration of FBS was 0.75%. Controls were treated with lipofectin alone. Luciferase activity was determined using a luciferase assay kit (Tropix, Bedford, MA) and shown as luciferase activity/unit protein.

Acknowledgements

The authors thank Dr. MaoJun Guo for his help in the synthesis of some of the bicyclic oxazaphospholidine nucleoside monomers.

References

1. Akhtar, S.; Agrawal, S. *Trends Pharm. Sci.* **1997**, *18*, 12.
3. Eckstein, F. *Annu. Rev. Biochem.* **1985**, *54*, 367.
2. Kronenwett, R.; Haas, R. *Ann. Hematol.* **1998**, *77*, 1.
4. Tang, J.-Y.; Roskey, A.; Li, Y.; Agrawal, S. *Nucleosides Nucleotides* **1995**, *14*, 985.
5. Koziolkiewicz, M.; Krakowiak, A.; Kwinkowski, M.; Boczkowska, M.; Stec, W. J. *Nucleic Acids Res.* **1995**, *23*, 5000.
6. Koziolkiewicz, M.; Wojcik, M.; Kobylanska, A.; Karwowski, B.; Rebowska, B.; Guga, P.; Stec, W. J. *Antisense Nucleic Acid Drug Dev.* **1997**, *7*, 43.
7. Hacia, J. G.; Wold, B. J.; Dervan, P. B. *Biochemistry* **1994**, *33*, 5367.
8. Hartmann, B.; Bertrand, H.-O.; Fermandjian, S. *Nucleic Acids Res.* **1999**, *27*, 3342.
9. Tamura, Y.; Miyoshi, H.; Yokota, T.; Makino, K.; Murakami, A. *Nucleosides Nucleotides* **1998**, *17*, 269.
10. Stec, W. J.; Wilk, A. *Angew. Chem., Int. Ed. Engl.* **1994**, *33*, 709.
11. Stec, W. J.; Grajkowski, A.; Kobylanska, A.; Darwowski, B.; Koziolkiewicz, M.; Misiura, K.; Okruszek, A.; Wilk, A.; Guga, P.; Boczkowska, M. *J. Am. Chem. Soc.* **1995**, *117*, 12020.
12. Iyer, R. P.; Yu, D.; DevIin, T.; Ho, N.; Agrawal, S. *J. Org. Chem.* **1995**, *60*, 5388.
13. Iyer, R. P.; Yu, D.; Ho, N.; Tan, W.; Agrawal, S. *Tetrahedron: Asymmetry* **1995**, *6*, 105.
14. Wang, J.-C.; Just, G. *Tetrahedron Lett.* **1997**, *38*, 3797.
15. Iyer, R. P.; Guo, M.-J.; Yu, D.; Agrawal, S. *Tetrahedron Lett.* **1998**, *39*, 2491.
16. Guo, M. J.; Yu, D.; Iyer, R. P.; Agrawal, S. *Bioorg. Med. Chem. Lett.* **1998**, *8*, 2539.
17. Yokuzaki, H.; Budillon, A.; Tortora, G.; Meissner, S.; Beaucage, S. L.; Miki, K.; Cho-Chung, Y. S. *Cancer Res.* **1993**, *53*, 868.
18. Nesterova, M.; Cho-Chung, Y. S. *Nature Med.* **1995**, *1*, 528.
19. Chen, L.; Agrawal, S.; Zhou, W.; Zhang, R.; Chen, J. *Proc. Natl. Acad. Sci. USA* **1998**, *95*, 195.
20. Bachelin, M.; Hessler, G.; Kurz, G.; Hacia, J. G.; Dervan, P. B.; Kessler, H. *Nature Struct. Biol.* **1998**, *5*, 271.
21. Furrer, P.; Billeci, T. M.; Donati, A.; Kojima, C.; Karwowski, B.; Sierzchala, A.; Stec, W.; James, T. L. *J. Mol. Biol.* **1999**, *285*, 1609.
22. Clark, C. L.; Cecil, P. K.; Singh, D.; Gray, D. M. *Nucleic Acids Res.* **1997**, *25*, 4098.
23. Agrawal, S.; Jiang, Z.; Zhao, Q.; Shaw, D. R.; Cai, Q.; Roskey, A.; Channavajjala, L.; Saxinger, C.; Zhang, R. *Proc. Natl. Acad. Sci. USA* **1997**, *94*, 2620.
24. Gao, W.-Y.; Han, F.-S.; Storm, C.; Egan, W.; Cheng, Y. C. *Mol. Pharmacol.* **1992**, *41*, 223.
25. Agrawal, S.; Zhang, X.; Cai, Q.; Kandimalla, E. R.; Manning, A.; Jiang, Z.; Marcel, T.; Zhang, R. *J. Drug Target.* **1998**, *5*, 303.
26. Benimetskaya, L.; Tonkinson, J. L.; Koziolkiewicz, M.; Karwowski, B.; Guga, R.; Zeltser, R.; Stec, W.; Stein, C. A. *Nucleic Acids Res.* **1995**, *23*, 4239.
27. Pisetsky, D. S.; Reich, C. F. *Life Sci.* **1993**, *54*, 101.
28. Krieg, A. M.; Yi, A. K.; Matson, S.; Waldschmidt, T. J.; Bishop, G. A.; Teasdale, R.; Koretzky, G. A.; Klinman, D. M. *Nature* **1995**, *374*, 546.
29. Zhao, Q.; Temsamani, J.; Iadarola, P. L.; Jiang, Z.; Agrawal, S. *Biochem. Pharmacol.* **1996**, *51*, 173.
30. Agrawal, S.; Zhao, Q. *Curr. Opin. Chem. Biol.* **1998**, *2*, 519.
31. Fearon, K. L.; Hirschbein, B. L.; Chiu, C.-Y.; Quijano, M. R.; Zon, G. *Oligonucleotides as Therapeutic Agents, Ciba Foundation Symposium 209*; John Wiley & Sons, Chichester, 1997; pp. 19–37.
32. Agrawal, S.; Tan, W.; Cai, Q.; Xie, X.; Zhang, R. *Antisense Nucleic Acid Drug Dev.* **1997**, *7*, 245.
33. Buczko, W.; Cierniewski, C.; Kobylanska, A.; Koziolkiewicz, M.; Okruszek, A.; Pawlowska, Z.; Pluskota, E.; Stec, W. J. *Pharmacol. Ther.* **1997**, *76*, 161.
34. Stec, W. J.; Cierniewski, C. S.; Okruszek, A.; Kobylanska, A.; Pawlowska, Z.; Koziolkiewicz, M.; Pluskota, E.; Maciaszek, A.; Rebowska, B.; Stasiak, M. *Antisense Nucleic Acid Drug Dev.* **1997**, *7*, 567.
35. Capaccioli, S.; DiPasquale, G.; Mini, E.; Mazzei, T.; Quattrone, A. *Biochem. Biophys. Res. Commun.* **1993**, *197*, 818.
36. Shen, L. X.; Kandimalla, E. R.; Agrawal, S. *Bioorg. Med. Chem.* **1998**, *6*, 1695.